

# Physically-based simulation of plant leaf growth

By Iris R. Wang\*, Justin W. L. Wan and Gladimir V. G. Baranoski



*A mathematical model is presented to simulate the growth of a plant leaf. The tissue in the leaf has been regarded as a viscous, incompressible fluid whose 2D expansion comes from the non-zero specific growth rate in area. The resulting system of equations are composed of the modified Navier-Stokes equations. The level set method is used to capture the expanding leaf front. Numerical simulations indicate that different portions of the leaf expand at different rates, which is consistent with the biological observations in the growth of a plant leaf. Numerical results for the case of the Xanthium leaf growth are also presented. A standard ray tracing technique is applied to produce an animation simulating the leaf growth process of three days. The key results with their physical and practical implications are discussed. Copyright © 2004 John Wiley & Sons, Ltd.*

KEY WORDS: plant; leaf; growth model; physically-based simulation; natural phenomena

## Introduction

Plant modelling and simulation play an important role in realistic image synthesis for outdoor scenes, forests, gardens, or even interior designs. Methods and techniques have been developed for various aspects of plant simulation. For instance, L-system was proposed to model plant morphology and plant growth,<sup>1</sup> in which plants are described as an arrangement of functional modules such as buds or leaves. Interactive modeling methods, which combine a rule-based approach with traditional geometric modeling techniques, have been used for generation of many branching objects such as flowers, bushes, and trees.<sup>2</sup> However, these growth models are for the plant as a whole rather than for the individual plant organs such as leaves. Rendering techniques for plant leaves using physically-based approaches have been developed.<sup>3,4</sup> The primary focus of these papers is to create images of static leaves. However, the modelling of growing plant leaves has not received much study in the computer graphics literature. In this paper, we propose a physically-based approach to model plant leaf growth based on a modification of the

incompressible Navier-Stokes equations.<sup>5</sup> A standard ray tracing technique is applied to produce an animation simulating the leaf growth process of three days.

Navier-Stokes equations were originally developed to describe the dynamics of fluid flow.<sup>5</sup> Recently, in computer graphics, Navier-Stokes equations have been successfully used in the animation of physical phenomena, for instance, water,<sup>6</sup> smoke,<sup>7</sup> cloud,<sup>8</sup> and fire,<sup>9</sup> which are either fluid or exhibiting the fluid behaviour and hence the Navier-Stokes equations are a natural approach.

Modelling the growth of plant leaves using the Navier-Stokes equations, however, is less obvious. For instance, it is more difficult to view a plant tissue as a continuum, since the relative size of the fundamental units, the cells, to a plant tissue is larger than that of the molecules to a fluid. Nevertheless, it is frequently found that the tissue or organ of interest consists of rather large number of cells. The growing region of a primary root of a Zea seedling consists of more than 250 000 cells.<sup>10</sup> As to the temporal aspects, the growth expansion of tissues is observed to be continuous. This is evident, for example, in the studies of root growth.<sup>11</sup> In leaves as well, growth appears to be smooth in time and with respect to spatial dimensions. This can be seen in time-lapse motion pictures of growing plant leaves.<sup>12</sup>

Another issue of applying the Navier-Stokes equations to modelling growth is that conservation of mass, which assumes that matter is neither created nor destroyed, does not hold. For plant growth, matter is

\*Correspondence to: Iris R. Wang, School of Computer Science, University of Waterloo, 200 University Avenue West, Waterloo, Ontario, Canada.  
E-mail: r5wang@uwaterloo.ca

created in cell divisions. In fact, we will show in the next section that the relative elemental growth rate is the divergence of the growth velocity field,  $\nabla \cdot u$ . For a plant element which is expanding,  $\nabla \cdot u$  is positive due to transport and biosynthesis.<sup>10</sup> This is in contrast with the classical modelling of incompressible fluids. We note that nonzero velocity divergence has recently been used in the modelling of explosion.<sup>13</sup>

The mathematical model we used to simulate the plant leaf growth is a two-dimensional model. The primary focus is on the growth in area of plant leaves. One of our future goals is to expand it to three dimensions and include the growth in thickness as well. At this stage, however, we emphasize the growth of its two-dimensional shape since the growth in thickness of a leaf can be considered negligible compared to the growth in area. For example, the average length and width of the soybean leaves are 14 cm and 10 cm,<sup>14</sup> respectively, whereas the average thickness is 166 microns.<sup>15</sup> In this paper, we model the growth of the plant leaf as an incompressible viscous flow. The system consists of the modified momentum equations from Navier-Stokes equations<sup>5,16</sup> and the equation of continuity based on the experimental data from.<sup>17-19</sup> We use the level set method of Osher and Sethian<sup>20</sup> to capture the expanding leaf edge.

Due to the absence of experimental data, we recognize that some biological growth factors such as chemical reaction between cells and genetic development have not been incorporated into our models. But we believe that as the experimental measurement improves as well as the biological growth of plant leaves is better understood, more accurate and complete information can be obtained and be incorporated into the proposed framework. Our model then can be refined and be used not just for animation in computer graphics but also to facilitate biological research for leaf growth.

## Modelling

The incompressible Navier-Stokes equations determine fluid motions by enforcing the conservation of momentum and mass. The resulting momentum and continuity equations can be written in dimensionless form as:

$$u_t + (u \cdot \nabla)u = \frac{1}{Re} \Delta u - \nabla p + f \quad (1)$$

$$\nabla \cdot u = 0, \quad (2)$$

where  $u$  is the fluid velocity vector,  $p$  is the pressure,  $f$  denotes body forces such as gravity, and  $Re$  is the Reynolds number which represents the viscosity of the fluids.<sup>5</sup> These equations have been used in the animations of various physical phenomena involving fluid, or fluid-like materials.<sup>6-9</sup>

In<sup>10</sup>, Silk and Erickson pointed out that many of the concepts and equations which have been used in the study of fluids can be applied to plant development. For plant growth, in particular, the growth of a leaf,  $u$  is identified with the growth velocity, and  $p$  is the pressure exerted by the growing cells. In growth modelling, mass is not conserved; in fact, it is increasing as the plant tissues grow. As a result, the continuity equation must be modified to accommodate the mass increase due to growth. In the next section, we discuss how the growth velocity and growth rate are used to model the local biosynthesis and transport rate in expanding tissue.

## Growth Rate

There is a long history of plant leaf growth study by biologists. In 1933, Avery<sup>17</sup> presented a systematic experimental approach to the study of the growth of *Nicotina tabacum* (tobacco). Later, Richards and Kavanagh<sup>18</sup> analyzed the data of Avery to study the distribution of the values of the relative growth rate in area. They also derived a mathematical formulation for plant leaf growth. Consider a small area defined by  $P_0, P_1, P_2$  and  $P_3$  inside the leaf region as shown in Figure 1(a). For convenience, we choose  $P_0$  as the origin and the polygon is a standard rectangular so that the area is  $\Delta x \times \Delta y$ . After a short time  $dt$ ,  $P_1$  at  $(\Delta x, 0)$  moves to a new position at  $(\Delta x + \frac{\partial u}{\partial x} \Delta x dt, \frac{\partial v}{\partial x} \Delta x dt)$  and similarly  $P_2$  at  $(0, \Delta y)$  moves to  $(\frac{\partial u}{\partial y} \Delta y dt, \Delta y + \frac{\partial v}{\partial y} \Delta y dt)$ . Then the new area can be computed by vector analysis as  $\Delta x \Delta y + (\frac{\partial u}{\partial x} + \frac{\partial v}{\partial y}) \Delta x \Delta y dt$ . Therefore, the relative growth rate (per unit time per unit area) is  $\frac{\partial u}{\partial x} + \frac{\partial v}{\partial y}$ , which is precisely the divergence of the growth velocity. Hence, the continuity equation (2) becomes

$$\nabla \cdot u = L(x, t), \quad (3)$$

where  $L(x, t)$  is the relative growth rate.

The field variable  $L$ , in general, is unknown. To produce a realistic simulation comparable to the real growth of plant leaves, we incorporate the real biological data<sup>17-19</sup> for  $L$  in our simulation. Since the different parts of the leaf's lamina might expand at different rates, Maksymowych<sup>19</sup> gave the local growth rates of the *Xanthium* leaf on small regions separated by veins.

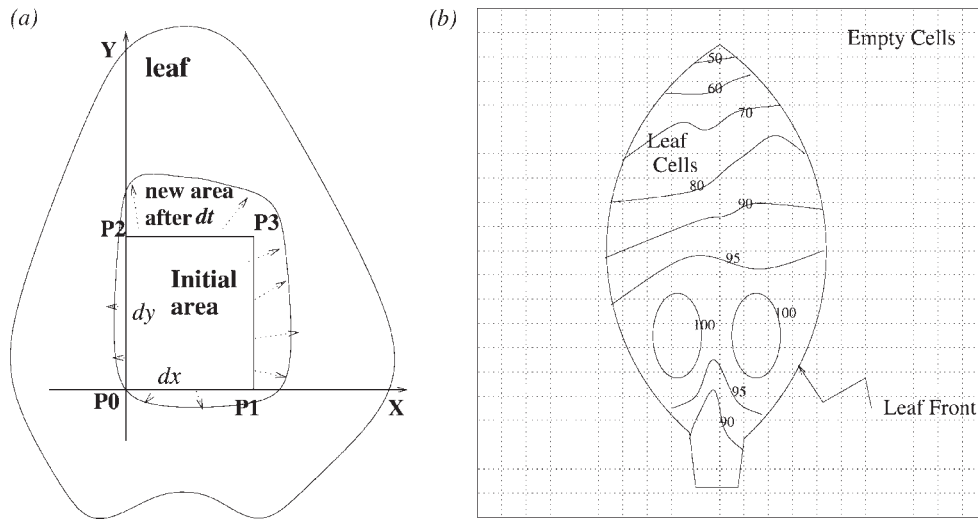


Figure 1. (a) Differential growth of a plant leaf in a short time  $dt$ . (b) Distribution of relative growth rate in area (redrawn from<sup>18</sup>).

Richards and Kavanagh,<sup>18</sup> on the other hand, represent growth rates by contour lines, as shown in Figure 1(b). The number on the curves indicate a percentage increase in area per day. For example, the curves marked 100 represent those of approximately the maximum rate. Then the curves marked 90 indicate that their rate are 90 percent of the curves marked 100. Even though these experimental data on different leaves are variable, we can still conclude that various parts of the leaf's lamina expand at different rates and the relative growth rate is lowest at tip of the leaf and increase in the basal direction.<sup>18,19</sup>

### Modified Momentum Equations

For plant leaf growth, we ignore any body forces (e.g. gravity) and only assume surface forces, which are typically expressed by the stress tensor,  $\sigma$ . Thus, the momentum equations can be written as:

$$u_t + (u \cdot \nabla)u + u(\nabla \cdot u) = \nabla \cdot \sigma.$$

To specify  $\sigma$ , we need to make several assumptions. First, we assume that biological tissues behave more like viscous than inviscid fluids.<sup>21</sup> Second, we assume that plant leaf growth is isotropic; i.e., there is no preferential direction for cell growth. This is consistent with the findings of Richards and Kavanagh for tobacco leaves<sup>18</sup> that as the leaf passes the very early growth stages, the

growth tends to be isotropic. We note that since the growth rates are different at different parts of a leaf, a non-uniform growth can still result even though the growth is isotropic. Under these assumptions, the surface forces given by the stress tensor can be modelled by

$$\nabla \cdot \sigma = -\nabla p + \frac{1}{3Re} \nabla(\nabla \cdot u) + \frac{1}{Re} \Delta u,$$

as for Newtonian fluids obeying the Stokes assumption.<sup>5</sup> Combining with the formula for the growth rate (3), we obtain the modified momentum equations for the plant leaf growth

$$u_t + (u \cdot \nabla)u + Lu = -\nabla p + \frac{1}{3Re} \nabla L + \frac{1}{Re} \Delta u. \quad (4)$$

In summary, the modified continuity equation (3) and the modified momentum equations (4) form the basis of our growth model for plant leaves.

### Outline of Algorithm

Our model presented in this paper consists of a fluid mechanical component describing the two-dimensional outgrowth of plant leaves and a diffusion-advection component determining the spatio-temporal distribution of the growth rate. We solve the discrete equations

corresponding to (3) and (4) over time. The growth velocity field, updated in each time step, will be used to update the leaf front. The expanding leaf edge is then passed to a graphics ray tracer for rendering. The final animation is composed of frames generated in each time step.

The algorithm can be summarized in the following major steps:

- Step 1.* Model the static background as a staggered grid, inside which model the initial shape of a leaf. Then, for each simulation time step,
- Step 2.* Update the velocity field by solving (3) and (4) using the projection method by Chorin.<sup>22</sup>
- Step 3.* Update the shape of the leaf using the new velocity field.
- Step 4.* Render one frame of the updated shape of the leaf using a standard ray-tracer. Go to *Step 2.*

These steps are described in detail in the following sections.

## Initial Geometric Set-Up

In our mathematical model, the motion of the liquid is described by the evolution of two dynamic field variables, velocity and pressure. In two dimensions, the velocity vector is composed of the horizontal component  $u$  and the vertical component  $v$ . On a Cartesian grid  $D$ , we locate the pressure variables  $p$  in the cell centers,  $u$  on the midpoints of the vertical cell edges, and  $v$  on the midpoints of the horizontal cell edges. As a result, each of the discrete values of  $u$ ,  $v$  and  $p$  is shifted half a cell length to each other. This staggered arrangement of the unknowns can prevent possible pressure oscillations which could happen if we evaluated them at the same grid points.<sup>23</sup>

To represent the shape of the leaf edge, we introduce another field variable  $\phi$  located in the center of each cell. We define

$$\phi(x, t = 0) = d, \tag{5}$$

where  $d$  is the signed distance from the position  $x$  to the leaf front. Hence the leaf edge is determined by the set  $\{x|\phi(x, t) = 0\}$ . This function  $\phi$  naturally defines grid points that are inside and outside of the leaf; the grid point is inside if  $\phi > 0$ , and outside if  $\phi < 0$ . We denote the leaf region by  $\Omega$  and the region outside of the leaf by  $\Omega^c$ . The computation of the pressure and velocity variables is confined to the leaf region. However, the computation of  $\phi$  will be on the entire grid  $D$ .

## Update of the Velocity Field

The crucial part in implementing our mathematical model is to solve (3) and (4) for the velocity field over time. Its numerical computation can be further divided into four steps. First, the size of the grid cell and the Euler-integration time step should be chosen to ensure the numerical stability. Second, the values of pressure and velocity which are outside of the leaf but adjacent to the grid cells inside of the leaf must be specified to satisfy the boundary conditions. Third, equation (3) is enforced by taking the divergence of equation (4) which then yields a Poisson equation for the pressure. Finally, we update the velocity field using the finite difference method.

### Boundary Conditions

As we decompose the whole domain  $D$  into two regions, the velocity and pressure values of the grid cells outside of and away from the leaf edge are set to zero. For those near the edge, the values are set to be consistent with the boundary conditions. These boundary conditions determine the velocity of the expanding leaf front. Intuitively, as the leaf grows, the growth velocity should not change in the direction normal to the boundary. Hence the outflow boundary conditions are used:

$$\frac{\partial}{\partial n} u_n = 0 \quad \frac{\partial}{\partial n} u_\tau = 0 \tag{6}$$

where  $u_n$  is the component of velocity in the exterior normal direction and  $u_\tau$  is the component of velocity in the tangential direction to the boundary. These boundary conditions set the normal derivatives of  $u_n$  and  $u_\tau$  to zero at the boundary. Thus, the leaf will grow outward with the same speed and in the same direction. In our model, we assume the air dynamics has a negligible effect on the leaf growth. The values of pressure on the boundary cell are set to zero.

### Discretization in Time

When solving the evolution of the velocity over time, we need to perform the time discretization on the equations (3) and (4). In order to maintain the stability of our numerical algorithm, stability conditions must be imposed on the step size  $\delta t$  and the cell size  $\delta x \times \delta y$ . We use an adaptive stepsize control based on the result from<sup>24</sup>

by selecting  $\delta t$  for the next time step so that each of the following is satisfied:

$$\delta t = \tau \min \left( \frac{Re}{2} \left( \frac{1}{\partial x^2} + \frac{1}{\partial y^2} \right)^{-1}, \frac{\partial x}{|u_{\max}|}, \frac{\partial y}{|v_{\max}|} \right). \quad (7)$$

The factor  $0 < \tau \leq 1$  is a safety factor,  $|u_{\max}|$  and  $|v_{\max}|$  are the maximal absolute values of the velocities inside the leaf domain  $\Omega$ . The restriction of  $\delta t |u_{\max}|$  must be smaller than the cell size is called Courant-Friedrichs-Lewy (CFL) condition. Under such a restriction no grid point can move further than a cell size in one time step size. Beginning at time  $t=0$  with initial values of velocity, time is increased by  $\delta t$  in each step until the final time is reached. At time step  $n+1$  the field variables are computed based on their values at previous time step  $n$ .

We rewrite the equation (4) in discretized form as

$$u^{n+1} = U^n - \delta t \nabla p^{n+1}$$

where

$$U = u + \delta t \left( \frac{1}{Re} \Delta u - (u \cdot \nabla)u - Lu + \frac{1}{3Re} \nabla L \right). \quad (8)$$

In equation (8), the velocity field at time step  $n+1$  can be computed once the corresponding pressure is known. The problem can be solved by using the Laplacian operator to couple the pressure changes to the velocity changes in the continuity equation (3), which gives

$$\nabla^2 p = \frac{1}{\delta t} (\nabla \cdot U - L) \quad (9)$$

where  $\nabla^2 p$  is the Laplacian of the pressure.

From equation (9), we form a symmetric and positive definite linear system  $AP = b$  where  $P$  is the vector of unknown pressures inside the leaf region,  $b$  is the vector formed by the values of the right-hand side of (9), and  $A$  is the discrete Laplacian matrix. We note that the irregular shape of the leaf only affects the positions of the nonzero entries but does not destroy the symmetric structure of  $A$ . Hence, the linear system can be solved efficiently using the conjugate gradient method.<sup>25</sup>

After the new pressures at time step  $n+1$  have been determined, the velocities in each cell are computed by (8). The new velocity field can then be used to update the distance function  $\phi$  to capture the expanding leaf edge.

## Leaf Expansion

As we have described above, the initial shape of the leaf is given by the zero level set of the signed distance

function. This function  $\phi$  is also called a level set function which was first introduced by Osher and Sethian<sup>20</sup> to capture moving front. Since then, this topologically robust interface capturing method has been used to track interfaces in a wide variety of applications. The main idea of the level set method is to embed the moving interface as the zero level set (cf. (5)). Once we have known the velocity at which the front moves, we will update  $\phi$  using the following equation

$$\phi_t + (u \cdot \nabla)\phi = 0, \quad (10)$$

so that the leaf front will always be equal to the zero level set of  $\phi$ . Here the velocity  $u$  is given by the growth velocity computed from (8). In order to get a more accurate update, we use the upstream second-order accurate approximation<sup>26</sup> for the convective term  $(u \cdot \nabla)\phi$  above.

The evolution equation (10) for  $\phi$  does not keep  $\phi$  as an exact distance function over time. Steep or flat gradients can develop in  $\phi$  as it moves. A common technique to fix this problem is to reinitialize  $\phi$ .<sup>16</sup> Denote the level set function representing the current leaf edge by  $\phi_0$ ; *i.e.*, the zero level set of  $\phi_0$  gives the leaf edge. To construct a function  $\phi$  whose zero level set is the same as  $\phi_0$  and that it is the signed distance function, we solve the following problem to steady state:

$$\phi_t = S_\varepsilon(\phi_0)(1 - |\nabla\phi|) \quad \text{where} \quad S_\varepsilon(\phi) = \frac{\phi}{\sqrt{\phi^2 + \varepsilon^2}}. \quad (11)$$

Thus, the distance values away from the interface will converge to  $|\nabla\phi| = 1$ .

In our computation, the value of  $\varepsilon$  is set as the size of one grid cell. Typically, three to four time steps would be sufficient. Afterwards, the contour of the leaf edge will be passed to our standard ray tracer for rendering one frame of the current shape of the leaf.

## Verification and Results

The growth model developed in this paper has been tested on the growth of two types of leaves, Xanthium and golden pothos. For the former, we carry out a quantitative analysis of our model; we simulate the growth of a Xanthium leaf using biological growth data and then compare the simulated results with the experiments. For the latter, we give a qualitative study;

we simulate the growth of a golden pothos leaf for three days. The simulation is presented as an animation available at <http://www.curumin.uwaterloo.ca/~r5wang>.

The spatial and temporal growth of a plant leaf is not uniform in general, and hence a realistic growth model needs to be able to capture these effects. In<sup>19</sup>, an experimental study of the growth of the *Xanthium* leaves was carried out. The absolute (global) rates of growth in area were recorded daily. However, the rates are plotted against the *leaf plastochron index* (LPI), defined as:

$$LPI = \frac{\log L_n - \log 10}{\log L_n - \log L_{n+1}}, \quad (12)$$

where  $n$  denotes the  $n$ th oldest leaf of a *Xanthium* plant and  $L_n$  is the length of leaf  $n$  (measured in mm). The LPI of a leaf essentially indicates the age of that leaf relative to the time when it was 10 mm long. In this study, it has been observed that various parts of the leaf's lamina expand at different rates, depending on their distance from the tip and the age of the leaf. The relative growth rate is lowest at the tip of the leaf and increases in the basal direction, thus conforming to the basipetal pattern of expansion.

The relative rates of increase in area at different parts of a *Xanthium* leaf were obtained by marking experiments<sup>17</sup> on the leaf surface. We simulate the growth of the *Xanthium* leaf for LPI=0.74, 2.64, and 4.18. The relative (local) grow rates from<sup>19</sup> are used to define the field variable  $L$  in (3). We compare the absolute growth rates of our simulated results with the experimental findings given in<sup>19</sup>.

As shown in Table 1, our simulated results are in good agreement with the experimental results. We remark that computer solutions are less predictable than the physical phenomena. Exact quantitative match would be unrealistic since our model does not use all the biological information (e.g. light, temperature, chlorophyll concentration, etc). One also needs to take into account the noise in measurement, especially for small values. Nevertheless, as observed in Table 1, the simu-

| LPI  | Experimental data | Simulation result |
|------|-------------------|-------------------|
| 0.74 | 0.34              | 0.61              |
| 2.64 | 6.6               | 6.20              |
| 4.18 | 10.7              | 10.3              |

**Table 1. The absolute growth rates of a *Xanthium* leaf when LPI = 0.74, 2.64, and 4.18**

| LPI  | Experimental data | Simulation result |
|------|-------------------|-------------------|
| 2.64 | 1.353             | 1.353             |
| 4.18 | 1.146             | 1.164             |

**Table 2. The length to width ratios of a *Xanthium* leaf growing from LPI = 2.64 to LPI = 4.18**

lated results are in the same order of magnitude as the experimental results. Furthermore, we also observe the temporal variation in the growth rates. The absolute growth rate in area is slower when the leaf is in the early developmental stage (LPI=0.74) and then increases as the leaf gets bigger (LPI=2.64); the rate eventually decreases as the leaf becomes mature (LPI = 4.18).

Our model is also able to capture the nonuniform spatial growth of the leaf. We start with the given shape of the *Xanthium* leaf when LPI = 2.64. Then we simulate the growth process until the length of the leaf is approximately equal to the length when LPI=4.18. The initial and the final length to width ratios are calculated and compared as shown in Table 2. We note that the growth in width is faster than the growth in length.

We have used our model to produce an animation simulating the leaf growth of golden pothos, also known as the 'devil's ivy', which is a hardy and fast growing trailing houseplant with heart shape leaves. The simulation sequence corresponding approximately to a growth period of three days is shown in Figure 2.

Each frame of the animation illustrating the growth of a plant leaf was rendered using ray tracing. The technique used to create the frames is similar to the one applied by Bloomenthal<sup>27</sup> and Hanrahan and Kruger.<sup>4</sup> It consists of mapping the leaf contour to a polygon. The colors of the polygon outside the leaf's contour are considered 'transparent' by the ray tracer.

Since we do not have the experimental data on the relative growth rate of area of golden pothos leaves, we defined the values of the field variable  $L$  in (3) depending on the distance from the leaf edge. This choice of growth rates is based on<sup>28</sup>, in which Erickson concluded that leaf expansion is largely isotropic, though the margins are somewhat anisotropic, and the direction of maximum expansion in the anisotropic growth was approximately parallel with the margin. Erickson also demonstrated that there was a general tendency for the center of the leaf to have higher rates than the margin.

The key parameters in the implementation are defined as follows: Reynolds number  $Re = 1000$ ,  $\tau = 0.5$ . For the

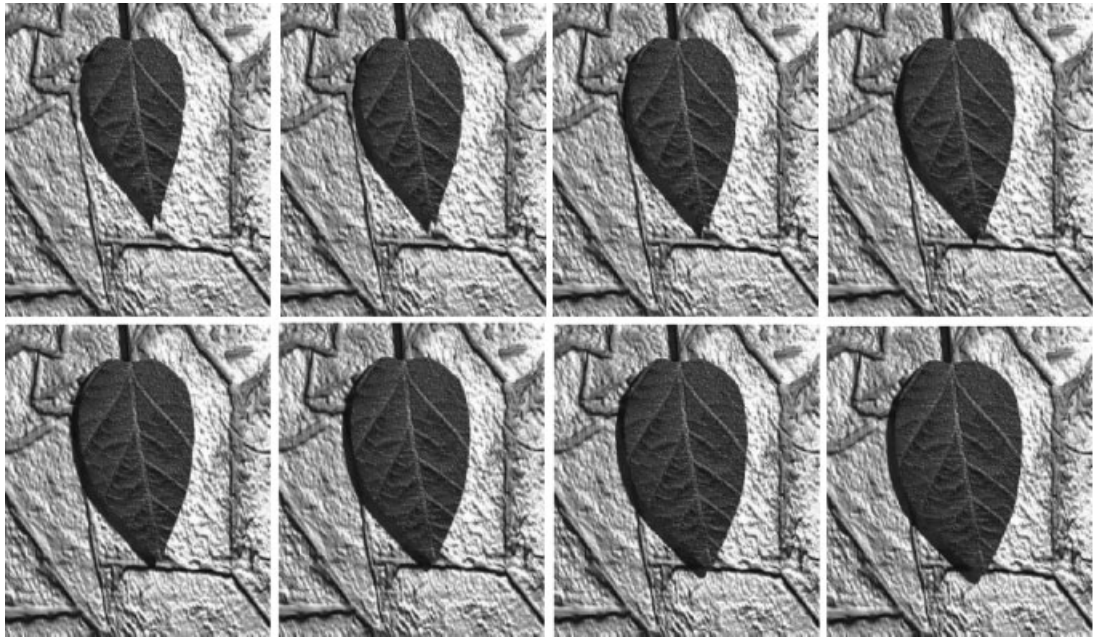


Figure 2. These eight pictures are the growing status at initial, 100th, 200th, 300th, 400th, 500th, 600th and 700th time steps. The animation corresponds approximately to three days in real life.

size of the domain  $D$ , we take  $n_x \times n_y = 200 \times 200$  for the numerical computation of the Xanthium leaves and  $n_x \times n_y = 500 \times 500$  for the rendering frames.

## Conclusion

We presented a mathematical model for simulating the growth of a plant leaf. We find that the experimental results, after comparing the modelled Xanthium leaf with the original one,<sup>19</sup> are consistent with the biological observations of the expansion in leaf morphology. Consequently we are confident that the presented model is operational and can be found useful in related applications such as botanical simulations. Our research is but an early step in developing a biophysically-based system of simulating plant growth. The difficulty in studying this problem stems from the lack of experimental data on spatial distribution of growth velocity and magnitude of the variable. In this paper, we have developed a model for simulating the growth in area of plant leaves. In the future, we plan to extend it to include the growth in thickness as well, which is an important parameter for biophysical rendering approaches. We will refine our model by integrating

more physical or biological factors once the availability of the experimental data on those factors are resolved.

## References

1. Prusinkiewicz P, Hammel MS, Mjolsness E. Animation of plant development. In *Proceedings of SIGGRAPH'93*, 1993; 351–360.
2. Lintermann B, Deussen O. Interactive modeling of plants. *IEEE Computer Graphics and Applications* 1999; **19**(1): 56–65.
3. Baranoski GVG, Rokne JG. Efficiently simulating scattering of light by leaves. *The Visual Computer* 2001; **17**: 491–505.
4. Hanrahan P, Krueger W. Reflection from layered surfaces due to subsurface scattering. In *Proceedings of SIGGRAPH'93*, 1993; 165–174.
5. Batchelor GK. *Introduction to Fluid Dynamics*. Cambridge University Press: Cambridge, UK; 1967.
6. Foster N, Fedkiw R. Practical animation of liquids. In *Proceedings of SIGGRAPH'01*, 2001; 23–30.
7. Fedkiw R, Stam J, Jensen HW. Visual simulation of smoke. In *Proceedings of SIGGRAPH'01*, 2001; 15–22.
8. Harris MJ, Baxter WV, Scheuermann T, Lastra A. Simulation of cloud dynamics on graphics hardware. In *Proceedings of the ACM SIGGRAPH/EUROGRAPHICS Conference on Graphics Hardware*. Eurographics Association: 2003; 92–101.

9. Nguyen DQ, Fedkiw R, Jensen HW. Physically based modeling and animation of fire. In *Proceedings of SIGGRAPH'02*, 2002; 721–728.
10. Silk WK, Erickson RO. Kinematics of plant growth. *J. Theor. Biol.* 1979; **76**: 481–501.
11. Goodwin RH, Avers CJ. Studies on roots III: an analysis of root growth in phlem pratense using photomicrographic records. *American Journal of Botany* 1956; **43**: 479–487.
12. Schmundt D, Lell M, Schurr U, Jahne B, Stitt M. Local orientation in the space-time domain as a tool for growth studies in plants. In *Proceedings of the International Conference on Spectroscopy and Optical Techniques in Animals and Plant Biology*. Munster 1996.
13. Feldman BE, O'Brien JF, Arikan O. Animating suspended particle explosions. *ACM Transactions on Graphics* 2003; **22**: 708–715.
14. Breece HT, Holmes RA. Bidirectional scattering characteristics of healthy green soybean and corn leaves in vivo. *Applied Optics* 1971; **10**(1): 119–127.
15. Hosgood B, Jacquemoud S, Andreoli G, Verdebout J, Pedrini G, Schmuck G. *Leaf Optical Properties Experiment 93*. Technical Report Report EUR 16095 EN, Joint Research Center, European Commission, Institute for Remote Sensing Applications, 1995.
16. Sussman M, Smereka P, Osher S. A level-set approach for computing solutions to incompressible two-phase flow. *J. Comput. Phys.* 1994; **114**: 146–159.
17. Avery GS Jr. Structure and development of the tobacco leaf. *American Journal of Botany* 1933; **20**(9): 565–592.
18. Richards OW, Kavanagh AJ. The analysis of the relative growth gradients and changing form of growing organism: illustrated by the tobacco leaf. *The American Naturalist* 1943; **77**(772): 385–399.
19. Maksymowych R. *Analysis of Leaf Development*. Cambridge University Press: Cambridge, UK; 1973.
20. Osher S, Sethian JA. Fronts propagating with curvature-dependent speed: algorithms based on Hamilton-Jacobi formulations. *J. Comput. Phys.* 1988; **79**: 12–49.
21. Dillon R, Othmer HG. A mathematical model for outgrowth and spatial patterning of the vertebrate limb bud. *J. Theor. Biol.* 1999; **197**: 295–330.
22. Chorin A. A numerical solution of the Navier-Stokes equations. *Math. Comp.* 1968; **22**: 745–762.
23. Griebel M, Dornseifer T, Neunhoffer T. *Numerical Simulation in Fluid Dynamics: A Practical Introduction*. SIAM 1998.
24. Tome MF, McKee S. Gensmac: a computational marker and cell method for free surface flows in general domains. *J. Comput. Phys.* 1994; **110**: 171–186.
25. Golub G, Van Loan C. *Matrix Computations*. Johns Hopkins: Baltimore, MD, USA; 1991.
26. Yavneh I. Coarse-grid correction for nonelliptic and singular perturbation problems. *SIAM J. Sci. Comput.* 1998; **19**(5): 1682–1699.
27. Bloomenthal J. Modeling the mighty maple. *Computer Graphics* 1985; **19**(3): 305–311.
28. Erickson RO. Relative elemental rates and anisotropy of growth in area: a computer programme. *J. Exp. Bot.* 1966; **17**: 390–403.